(ANPA Conference 2024)
ISSN: 2392-473X(Print), 2738-9537 (Online)

DOI: https://doi.org/10.3126/jnphyssoc.v10i1.72847

Effect of Thermal Quantum Species Screening Around Fuel Cell Anode Performance

Saddam Husain Dhobi,[1, a)] Jeevan Jyoti Nakarmi,[1, b)] Suresh Prasad Gupta,[2, c)] Kishori Yadav,[2, d)] and Ajay Kumar Jha[3, e)]

[1)] *Central Department of Physics, Tribhuvan University, Kirtipur, Kathmandu, Nepal.*
[2)] *Department of Physics, Patan Multiple Campus, Tribhuvan University, Lalitpur, Nepal*
[3)] *Department of Mechanical and Aerospace Engineering, Institute of Engineering, Pulchowk Campus, Tribhuvan University, Lalitpur, Nepal*

[a)] *Corresponding author: saddam@ran.edu.np*
[b)] *Electronic mail: nakarmijj@gmail.com*
[c)] *Electronic mail: guptasir@gmail.com*
[d)] *Electronic mail: yadavkishori70@gmail.com*
[e)] *Electronic mail: akjha@ioe.edu.np*

Abstract. The objective of this work is to develop a theoretical model, to study the effect of quantum species, activation potential, current density, and temperature/generated temperature on the performance of Pt/C catalysts in Proton Exchange Membrane Fuel Cells (PEMFCs). For this we modified Butler-Volmer equations and analyzing I-V characteristics, the observation shows lower activation potential of 40 mV yields better performance compared to 55 mV. The effect of temperature was observed showing that increased in temperatures can mitigate carbon support corrosion and decline the performance of PEMFCs. Also, increasing the electron flow per reaction cycle decreases the performance of PEMFCs by screening the flow of electrons. This result brings negative voltage and power, highlighting the complex interplay between these factors. The results underscore the importance of optimizing activation potential and managing temperature to enhance PEMFCs performance and longevity.

Received: August 26, 2024; **Revised**: October 8, 2024; **Accepted**: October 22, 2024

Keywords: PEMFCs, Butler-Volmer equations, I-V characteristics, Screening effect, Temperature.

INTRODUCTION

The design of a PEMFC is influenced by several factors, including gas distribution, moisture content in the Gas Diffusion Layer, heat exchange, and the properties of the membrane and catalyst. A critical aspect is moisture regulation in the membrane electrode assembly (MEA) [1]. According to Park et al., insufficient water content reduces ionic conductivity in the membrane and catalyst layer, increasing contact resistance between them. This impedes the removal of electrons at the reaction site, essential for the fuel cell's function. Conversely, excess water reduces catalytic sites for electrochemical reactions. Electrons are conducted away through the anode around an electrical circuit [2]. PEMFCs used in Unmanned Aerial Vehicles (UAVs) operate under high current density conditions, influenced by parameters like operating temperature, fuel supply pressure, and volumetric flow rates of air and fuel. A comprehensive optimization using the Taguchi Design of Experiment (DoE) method was conducted to optimize these conditions. MATLAB/Simulink simulations identified optimal conditions as 313 K operating temperature, 50 lpm fuel flow rate, 300 lpm air flow rate, and 1.5 bar fuel supply pressure. The contribution ratios to current density were 69.7% for temperature, 16.6% for supply pressure, 6.7% for fuel flow rate, and 0.9% for air flow rate [3]. In PEMFCs operation, oxidation occurs at the anode, where hydrogen gas (H_2) is oxidized to protons (H^+), releasing electrons. These electrons travel through an external circuit, generating current, while protons move through the membrane to the cathode. At the cathode, oxygen (O_2) from the air is reduced and combines with the protons and electrons to form water (H_2O) in an exothermic reaction [4].

PEMFCs have a simple structure consisting of two

porous conductive electrodes (anode and cathode), a polymer electrolyte, bipolar plates with gas flow channels, and an external electrical circuit. In a typical single cell, graphite plates with machined grooves provide pathways for hydrogen at the anode and air or oxygen at the cathode. Bipolar plates serve multiple functions, including electrical interconnection and structural support. Gas diffusion layers (GDLs) are placed between the bipolar plates and catalyst layers, facilitating gas distribution and acting as electrical contacts. Electrodes are thin catalyst layers where oxidation and reduction reactions occur [5, 6]. Understanding ionomer chemical degradation in PEMFCs has advanced through experimental testing and analysis. In-situ tests at open circuit voltage (OCV) reveal that reactant gas permeation and radical formation (e.g., hydrogen peroxide) occur even at 300 K. The potential profile within the membrane varies linearly, influencing the rate of oxygen reduction to hydrogen peroxide. The selectivity of peroxide formation over water generation varies with electrode potential and humidity [7–9]. Platinum nanocatalysts and their alloys are known for high catalytic activity, stability, durability, and selectivity for the cathodic reactions in energy conversion devices like PEMFCs. Protons produced from hydrogen oxidation at the anode are transported to the cathode, where they react in a multi-electron process to form water. The interfacial kinetics of these catalysts are crucial, with processes such as reactant adsorption, intermediate conversion, and product desorption enhancing efficiency and stability [10]. New M-N-C type catalysts are being studied for their kinetic ORR mechanisms and catalytic activity, with iron-based catalysts showing good activity and stability but causing membrane degradation via the Fenton reaction, prompting interest in cobalt compounds [11–14]. Bimetallic nitrides like Ti0.8Co0.2N show increased catalytic activity with cobalt incorporation, though still less than Pt/C in acidic mediums. Mo^{3+} in $Co_{0.6}Mo_{1.4}N$ enhances activity due to its hexagonal structure. MEA optimization involves blending catalysts with ultrapure water, Nafion, and isopropanol, affecting cost and performance. Reducing platinum group metal content in electrodes is a focus to lower costs for hydrogen-powered vehicles [15]. Nanoporous metals with continuous solid and pore phases ensure ion and electron flow, where pore size impacts mass transport and ion conduction. Advances in PEMFCs technology aim to reduce membrane costs and improve efficiency and durability, supported by mathematical models and experimental results [16].

The electrode in a PEMFC is essential for controlling reactant supply, proton and electron transport, water and heat management, and electrochemical reactions. Platinum (Pt) is the most popular catalyst due to its excellent activity, selectivity, and stability [17]. The structure of the electrode and the method of catalyst deposition significantly affect the rate of transport and electrochemical reactions. Catalysts can be coated on the membrane (CCM) or on the substrate. CCM electrodes generally perform better, especially at low Pt loadings, due to higher surface area in the catalyst layers, whereas CCS electrodes, although thinner and more porous, show significantly lower performance at low Pt loading due to catalyst penetration into the gas diffusion layer [18]. The GDL is a carbon-based porous component that bridges reactants and electrons in PEMFCs. Assembly pressure impacts GDL structure, affecting reactant distribution and PEMFCs performance. Variations in GDL properties due to assembly pressure can lead to uneven current density distribution and potential thermal damage to the MEA. Appropriate assembly pressure can improve PEMFCs output performance by optimizing the distribution of gases, water, heat, and electrons through the GDL [18].

Despite extensive research on PEMFCs, gaps remain in understanding specific activation potentials for Pt/C catalysts and the effects of thermal quantum species screening. Current studies reveal a gradient in d-spacing from the anode to the cathode, influenced by Pt particle scattering and hydration levels. Scattering data show that while small pores fill with water at lower current densities, larger pores only partially fill at higher saturation levels [19]. Particle size distributions obtained via the MaxEnt method highlight the complexity of water uptake in various pore sizes [20]. While much research has investigated temperature effects on PEMFC performance, the impact of thermal quantum species screening remains unexplored. This research aims to address this gap by interlinking screening parameters with the free electron gas model and incorporating them into the Helmholtz equation within the Butler–Volmer framework [1, 3, 21].

The thermal quantum species are defined as electrons, protons, and hydrogen molecules present in a thermal environment (1.17 eV to 1.24 meV) acting as non-monochromatic photons, which is created by the exothermic reaction in the presence of a catalyst at the electrode of PEMFC. These quantum species, formed within this thermally energized setting, interact and interfere with one another around the anode, significantly impacting the performance of the PEMFC. The behavior of these species, particularly their quantum interactions and interference, influences key factors such as proton transport, electron flow, and catalyst efficiency. Additionally, their interactions contribute to the overall thermal dynamics of the system, generating heat and causing temperature variations near the electrode. This temperature increase affects the fuel cell by enhancing particle mobility while also contributing to scattering effects around the electrode in self-generated temperature, scattering acts as within the laser field as the generated energy ranges from 1.17 eV to 1.24 meV, falling within the infrared (IR) spectrum., which can either improve or hinder the electrochemical processes within the cell. Effective man-

agement of these interactions is crucial for optimizing PEMFC performance and maintaining efficient energy conversion.

The dense formation of thermal quantum species, including electrons, protons, and hydrogen molecules, around the electrodes of the PEMFC creates screening effect. In this effect, the accumulation of these species near the electrode surface resists and hinders the free flow of both electrons and protons. As a result, the charged particles are screened/partially blocked from moving efficiently through the system. This resistance directly impacts the performance of the PEMFC, as it reduces the rate of proton transport through the membrane and impedes the electron flow through the external circuit, ultimately lowering the overall power output and energy efficiency of the cell. The screening effect, therefore, represents a significant challenge in optimizing PEMFC performance, as it can lead to energy losses and reduced operational efficiency.

METHODS AND MATERIALS

The output current and voltage of PEM fuel cell is defined by Butler–Volmer equation which is one of the most fundamental relationships in electrochemical kinetics. It describes how the electrical current on an electrode depends on the electrode potential, considering that both a cathodic and an anodic reaction occur on the same electrode [22]:

$$I = Ai_0 \left\{ \exp\left[\frac{\beta_a n_e F}{RT}(E - E_{\text{eq}})\right] - \exp\left[-\frac{\beta_c n_e F}{RT}(E - E_{\text{eq}})\right] \right\} \quad (1)$$

In more compact form

$$i = i_0 \left\{ \exp\left[\frac{\beta_a n_e F}{RT}\eta\right] - \exp\left[-\frac{\beta_c n_e F}{RT}\eta\right] \right\} \quad (2)$$

High-Overpotential Approximation $i = -i_0 \exp\left[\frac{\beta n F \eta}{RT}\right]$ for Large Cathodic Current and $i = i_0 \exp\left[\frac{(1-\beta) n F \eta}{RT}\right]$ for Large Anodic Current. In equations (1) and (2), I am electrode current measure in ampere, A is surface of the electrode, i is electrode current density defined as $i = \frac{I}{A}$, i_0 is exchange current density, E is electrode potential, E_{eq} is equilibrium potential, T is absolute temperature, n_e is number of electrons involved in the electrode reaction, F is Faraday constant, R is the universal gas constant, β_c and β_a is cathodic and anodic charge transfer coefficient which is dimensionless, η is activation overpotential defined as $\eta = (E - E_{\text{eq}})$. The value of $\beta_a + \beta_c = 1$, $\beta_a \approx \beta_c \approx \beta = 0.5$ [22]. In fuel cells, the movement of electrons through the external circuit and protons through the membrane for a single cell generates a voltage difference between the cell terminals and is given as

$$V_{\text{cell}} = E_{\text{Nernst}} - V_{\text{act}} - V_{\text{ohm}} - V_{\text{conc}} \quad (3)$$

Here, E_{Nernst} is the cell thermodynamic potential drop or initial voltage, V_{act} is activation polarization voltage, V_{ohm} is the ohmic polarized voltage of cell resistance and V_{conc} concentration polarization. The E_{Nernst} of equation (3) is calculated using Nernst equation as [23],

$$E_{\text{Nernst}} = \frac{\Delta G}{2F} + \frac{\Delta S}{2F}(T - T_{\text{ref}}) + \frac{RT}{2F}\left[\ln(P_{\text{H}_2}) + \frac{1}{2}\ln(P_{\text{O}_2})\right] \quad (4)$$

Here, ΔG is the change in the free Gibbs energy, F is the constant of Faraday, ΔS is the change of entropy of the reaction, R is the universal constant of the gases and P_{H_2} and P_{O_2} are the partial pressures of hydrogen and oxygen, respectively. T and T_{ref} denote the cell operating temperature and the reference temperature, respectively. Haji studied PEMFC voltage and current using $E^0 = 1.229$ V, $\Delta S = 163.23 J/molK$, n =2, F = 96485.35 C/mol, T_{ref} = 298.15 K, R = 8.314 J/molK reported by Akimoto and Okajima [24]. The activation polarizations of equation (3) is directly proportional to the increase in current flow and are defined as,

$$\eta_{\text{act}} = \frac{RT}{\alpha n F}\ln\left(\frac{i}{i_0}\right) \quad (5)$$

Here, α the charge transfer coefficient and this loss are due to slow electrochemical reactions at the electrode surface. The ohmic polarization varies with the increase in current due to the constant nature of fuel cell resistance and is defined as

$$\eta_{\text{ohm}} = IR_c \quad (6)$$

Here, R_c is the cell resistance and ohmic polarization resistance to the flow of ions in the electrolyte and flow of electrons through the electrodes and the external electrical circuit. The concentration losses take place due to the entire range of current density and are defined as

$$\eta_{\text{con}} = \frac{RT}{nF}\ln\left(1 - \frac{i}{i_L}\right) \quad (7)$$

Here, i_L is the limiting current density, the potential drop due to the drop in the initial concentration of the bulk of the fluid in the surroundings. Now from equation (3) on putting the value we get

$$V_{\text{cell}} = E_0 + \frac{\Delta S}{2F}(T - T_{\text{ref}}) + \frac{RT}{2F}\left[\ln(P_{\text{H}_2}) + \frac{1}{2}\ln(P_{\text{O}_2})\right] - \frac{RT}{2\alpha F}\ln\left(\frac{i}{i_0}\right) - iR_c - \frac{RT}{2F}\ln\left(1 - \frac{i}{i_L}\right) \quad (8)$$

Since,$\Delta G = nFE, n_e = n = 2$ Now total electrical power generated by a PEMFCs is obtained as

$$P = V_{\text{cell}} \cdot i = i_0 \left\{ \exp\left[\frac{2\beta_a F}{RT}\eta\right] - \exp\left[-\frac{2\beta_c F}{RT}\eta\right] \right\} \times \left\{ E_0 + \frac{\Delta S}{2F}(T - T_{\text{ref}}) + \frac{RT}{2F}\left[\ln(P_{H_2}) + \frac{1}{2}\ln(P_{O_2})\right] - \frac{RT}{2\alpha F}\ln\left(\frac{i}{i_0}\right) - iR_c - \frac{RT}{2F}\ln\left(1 - \frac{i}{i_L}\right) \right\} \quad (9)$$

Since there form quantum species (electrons, protons and hydrogen) round the electron cause the current production in circuit of PEMFCs. The electron formed around electrode is free and the number density is given as$\Delta n = D(E_F)eV$, where eV the change of the electron concentration and induced charge density is given as $\rho_{ind} = e\Delta n = e^2 D(E_F)V$, where density of states at the fermi energy of a three dimensional free electron gas is given as $D(E_F) = \frac{3n}{2}E_F$. For induced charge density the Helmholtz equation can be written as

$$\nabla^2 V - \frac{3e^2 n}{2\varepsilon_0 E_F}V = -\frac{e\delta(\mathbf{r} - \mathbf{r}')}{\varepsilon_0} \quad (10)$$

Ans also screening parameters with the Thomas-Fermi screening obtained as $k_s^2 = \frac{3e^2 n}{2\varepsilon_0 E_F} = \frac{3^{1/3} m e^2 n^{1/3}}{\varepsilon_0 \hbar^2 \pi^{4/3}}$. This give $n = \frac{\pi^4 k_s^6}{3}$ which is the relation of screening parameters and electron density. If we considered n is number of electrons produces in complete reaction cycle we have form this equation to (2) we get

$$i_s = i_0 \left\{ \exp\left[\frac{\beta_a F}{RT}\frac{\pi^4 k_s^6}{3}\eta\right] - \exp\left[-\frac{\beta_c n_e F}{RT}\frac{\pi^4 k_s^6}{3}\eta\right] \right\} \quad (11)$$

Now the equation with screening parametric is modified as

$$P = i_0 \left\{ \exp\left[\frac{\beta_a F}{RT}\frac{\pi^4 k_s^6}{3}\eta\right] - \exp\left[-\frac{2\beta_c F}{RT}\frac{\pi^4 k_s^6}{3}\right] \right\} \times \left\{ E_0 + \frac{\Delta S}{2F}(T - T_{\text{ref}}) + \frac{RT}{2F}\left[\ln(P_{H_2}) + \frac{1}{2}\ln(P_{O_2})\right] - \frac{RT}{2\alpha F}\ln\left(\frac{i}{i_0}\right) - iR_c - \frac{RT}{2F}\ln\left(1 - \frac{i}{i_L}\right) \right\} \quad (12)$$

RESULTS AND DISCUSSION

The activation potentials of 55 mV and 40 mV for Pt/C catalysts were obtained from the work of [25], who studied high-entropy materials as emerging electrocatalysts for hydrogen production through low-temperature water electrolysis. The I-V characteristics were analyzed using a modified Butler-Volmer equation, incorporating a screening parameter, as shown in Figure 1. The observed behavior in Figure 3 can be attributed to the generation and flow of electrons during a single cyclic reaction within a nanoscale section of the electrode. As the current density increases, the voltage decreases. This decrease is due to an increase in the charge transfer coefficient, which correlates with an increase in the power output as the current density rises. While this trend is generally consistent, there is a notable deviation around a current density of 0.47 mA/cm², where both power and voltage exhibit a peak. This peak is caused by a screening effect as well as electron interference in the presence of non-monochromatic photons generated around the electrode of PEMF, which occurs between the equilibrium and surface electrons formed around the electrode in the PEMFCs. The screening effect impedes the flow of electrons, leading to a temporary increase in both voltage and power. However, once the current density surpasses this critical point, the flow of electrons sharply increases, causing the voltage to decrease again, as the usual electron barrier formation takes place.

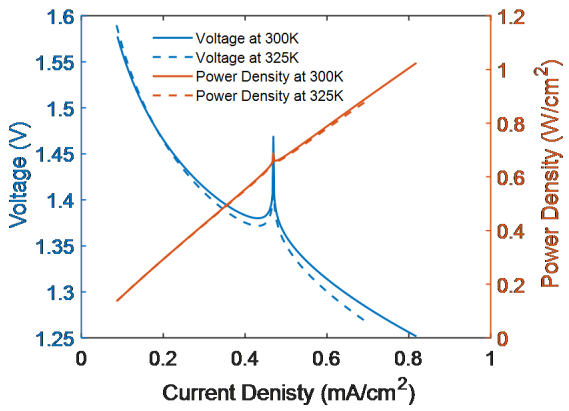

FIGURE 1. IV characteristic at 55 mV with 2 electrons per nano sec

Additionally, both power and voltage are influenced by temperature. The power output at 300 K is observed to be higher than at 325 K, which aligns with the findings [26, 27]. When examining the voltage as a function of current density, it is evident that at lower current densities, the voltage at the lower temperature (300 K) is also lower. However, as the current density increases, the voltage at the higher temperature (325 K) becomes lower, while the voltage at the lower temperature increases, as shown in Figure 1. This demonstrates that temperature plays a crucial role in determining both power and voltage. The observed effects are due to the influence of temperature on electron behavior. At higher temperatures, the electrons

formed are more affected by thermal agitation, leading to a decrease in both power and voltage. This decrease is a result of the combined effects of temperature and the previously mentioned screening effect, which together reduce the overall performance of the system. For the formation of four electrons per section, with an activation potential of 55 mV for Pt/C, the behavior is illustrated in Figure 2. In this case, the peak in power is shifted towards a lower current density region, and the nature of both power and voltage is consistent with the findings [28]. The shift and the observed behavior are primarily due to the screening effect as well as electron interference in the presence of non-monochromatic photons generated around the electrode of PEMF. However, in the scenario where four electrons are formed in a single cyclic reaction, the power output is higher as the current increases, and the screening effect is less pronounced compared to the formation of two electrons in a single system.

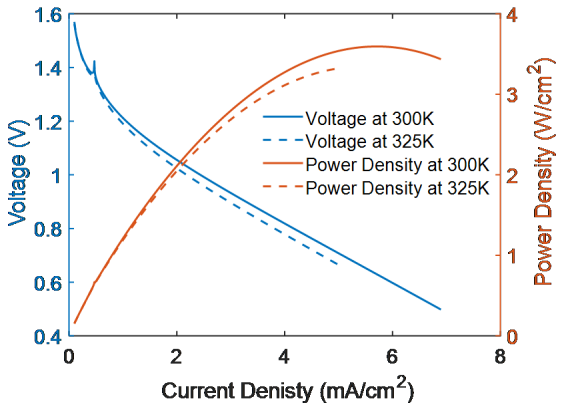

FIGURE 2. IV characteristic at 55 mV with 4 electrons per nano sec

Similar to the observations in Figure 1, the voltage and power at different temperatures exhibit a comparable trend. However, in the system involving the formation of four electrons per reaction, both the power and voltage are higher compared to the system with two-electron formation. This difference highlights the impact of electron formation on the overall system performance. Specifically, the increased electron formation in a single reaction leads to a higher energy output, resulting in greater power and voltage. In Figure 2, the voltage decreases more sharply in the system with four-electron formation compared to the system with two-electron formation. Despite this sharp decrease, the overall power trend remains consistent across both systems, although it diverges in magnitude. The decrease in voltage with increasing temperature, as reported [29], is more pronounced in the four-electron system, emphasizing the influence of thermal effects on electron behavior. Figure 3 provides a clear illustration of the combined effects of screening and temperature on power and voltage. The trends observed in this figure are markedly different from those seen in previous experimental work, likely due to the complex interplay between screening effects and temperature variations. In this context, the screening effect refers to the phenomenon where the electric field created by the electrons near the electrode surface reduces the effective force on other electrons, thus impeding their flow. One particularly noteworthy observation in Figure 3 is the occurrence of negative voltage and negative power. This phenomenon suggests that, under certain conditions, the system experiences a reverse bias where the direction of current flow is opposite to the expected direction. The presence of negative power indicates that the system is absorbing energy rather than delivering it, which could be attributed to the enhanced screening effect when a higher number of electrons are formed in a single reaction.

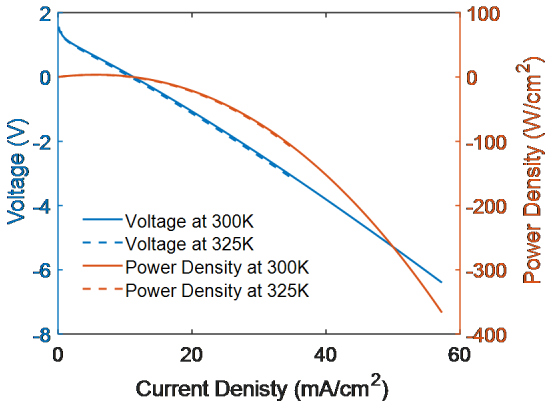

FIGURE 3. IV characteristic at 55 mV with 6 electrons per nano sec

The significance of negative power and negative voltage lies in the implications for system stability and efficiency. When the screening effect becomes more pronounced, it increases the resistance to electron flow, leading to a decrease in voltage and, eventually, the emergence of negative voltage. This reverse voltage, in turn, results in negative power, meaning that the system is effectively consuming energy. This behavior can be detrimental to the overall performance of the system, as it reduces the efficiency of energy conversion and may lead to operational instability. The formation of more electrons in a single reaction enhances the screening effect around the electrons, which in turn resists electron flow. This resistance manifests as a decrease in voltage and the potential emergence of negative voltage and power. Understanding and mitigating these effects is crucial for optimizing the performance of electrochemical systems, particularly in scenarios involving high electron formation rates.

Figure 4 illustrates the relationship between voltage, power, and current density for a Pt/C electrode with an ac-

tivation potential of 40 mV. The behavior observed in this figure closely mirrors the trends shown in Figure 3, particularly regarding the influence of temperature and current density on the system's performance. At a lower current density, the voltage at 325 K is higher than that at 300 K. This initially counterintuitive result can be attributed to the screening effect, which plays a significant role in the two-electron system. At lower temperatures, the screening effect is less pronounced, allowing electrons to flow more freely. However, as the temperature increases to 325 K, the screening effect becomes stronger, which initially increases the resistance to electron flow, leading to a higher voltage.

Similar to the observations in Figure 1, the voltage and power at different temperatures exhibit a comparable trend. However, in the system involving the formation of four electrons per reaction, both the power and voltage are higher compared to the system with two-electron formation. This difference highlights the impact of electron formation on the overall system performance. Specifically, the increased electron formation in a single reaction leads to a higher energy output, resulting in greater power and voltage. In Figure 2, the voltage decreases more sharply in the system with four-electron formation compared to the system with two-electron formation. Despite this sharp decrease, the overall power trend remains consistent across both systems, although it diverges in magnitude. The decrease in voltage with increasing temperature, as reported [29], is more pronounced in the four-electron system, emphasizing the influence of thermal effects on electron behavior. Figure 3 provides a clear illustration of the combined effects of screening and temperature on power and voltage. The trends observed in this figure are markedly different from those seen in previous experimental work, likely due to the complex interplay between screening effects and temperature variations. In this context, the screening effect refers to the phenomenon where the electric field created by the electrons near the electrode surface reduces the effective force on other electrons, thus impeding their flow. One particularly noteworthy observation in Figure 3 is the occurrence of negative voltage and negative power. This phenomenon suggests that, under certain conditions, the system experiences a reverse bias where the direction of current flow is opposite to the expected direction. The presence of negative power indicates that the system is absorbing energy rather than delivering it, which could be attributed to the enhanced screening effect when a higher number of electrons are formed in a single reaction.

As the current density increases, the trend reverses, and the voltage at 300 K surpasses that at 325 K. This reversal occurs because, at higher current densities, the screening effect at the higher temperature (325 K) becomes more dominant, impeding electron flow more significantly. Consequently, the voltage at 325 K drops

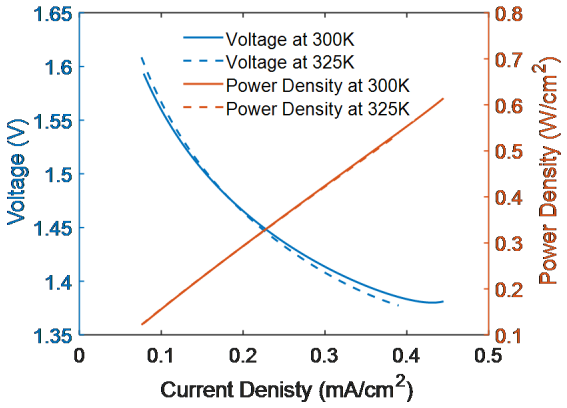

FIGURE 4. IV characteristic at 40 mV with 2 electrons per nano sec

below that at 300 K. A similar pattern is observed in the power output, where the power at 300 K is consistently higher than at 325 K, particularly in the higher current density region. The exchange of voltage behavior in the lower current density region due to the screening effect is particularly notable in the two-electron system. The screening effect refers to the interaction between the electric fields of closely spaced electrons, which can hinder their movement. At lower current densities, this effect is more prominent at higher temperatures, leading to the observed exchange in voltage behavior between 300 K and 325 K. This phenomenon aligns with findings from [30], who reported similar results in their studies. The consistency between these findings suggests that the interplay between temperature, current density, and the screening effect is a fundamental aspect of the behavior in Pt/C electrodes, particularly in systems involving the formation of two electrons per reaction. The I-V characteristics, as depicted in Figure 5, were analyzed using a modified Butler-Volmer equation that incorporates a screening parameter. The behavior observed in Figure 5 is attributed to the production and flow of two electrons in a single cyclic reaction within a nanoscale section. As the current density increases, the voltage decreases, which is associated with an increase in the charge transfer coefficient. Concurrently, the power increases with the rising current density. This trend is generally consistent; however, around 0.47 mA/cm², both the power and voltage exhibit a peak. This peak arises due to the screening effect between the equilibrium and surface electrons formed around the electrode in a PEMFC. The screening effect impedes the flow of electrons, causing an increase in voltage and power. However, as the current density continues to increase beyond this critical point, the flow of electrons sharply increases due to the screening effect as well as electron interference in the presence of non-monochromatic photons generated around the electrode

of PEMF, leading to a subsequent decrease in voltage as the normal electron barrier forms.

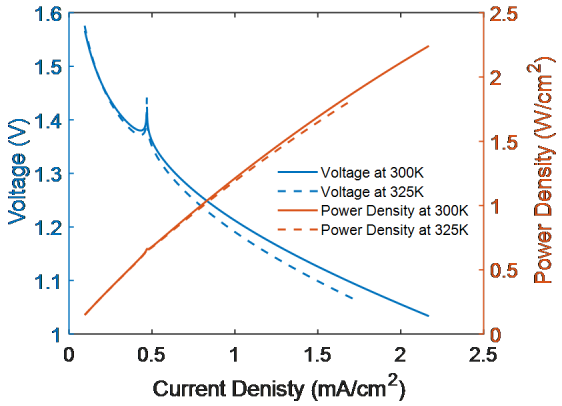

FIGURE 5. IV characteristic at 40 mV with 4 electrons per nano sec

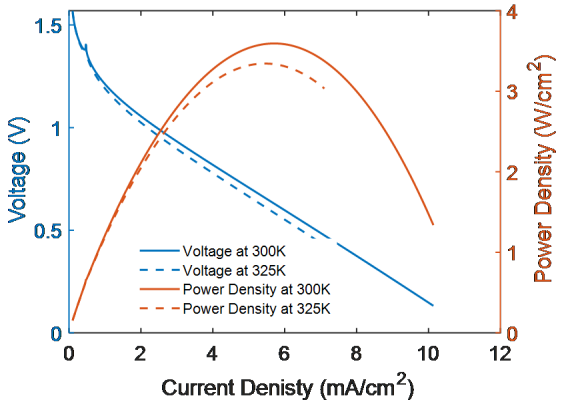

FIGURE 6. IV characteristic at 40 mV with 6 electrons per nano sec

Temperature also significantly influences both power and voltage. The power output at 300 K is higher than at 325 K, which is consistent with findings from previous studies. At lower current densities, the voltage at the lower temperature (300 K) is lower, but as the current density increases, the voltage at the higher temperature (325 K) becomes lower, while the voltage at the lower temperature rises, as shown in Figure 5. This indicates that temperature plays a crucial role in determining power and voltage. The observed decrease in power and voltage at higher temperatures can be attributed to the combined effects of temperature and screening. At higher temperatures, the formed electrons are more affected, leading to a decrease in both power and voltage. This behavior is similar to what is seen in Figure 1 for an activation potential of 40 mV, as compared to 50 mV. The behavior associated with the formation of six electrons per section, with an activation potential of 40 mV for the Pt/C electrode, is depicted in Figure 4. This behavior is analogous to that shown in Figure 2, but with some key differences. The most notable change is that the peak in power and voltage shifts toward a lower current density region. This shift is similar to the findings reported [31], where the impact of electron formation and screening effects was thoroughly examined. The observed shift is largely due to the screening effect, which plays a crucial role in modulating the system's response.

In systems where six electrons are formed in a single cyclic reaction, the power increases with rising current density, although the screening effect is less pronounced compared to systems where only four electrons are formed. This reduction in screening effect for the six-electron system leads to a smoother increase in power and a corresponding shift of the peak towards lower current densities. Similar trends are observed in Figure 1, where voltage and power at different temperatures exhibit comparable behaviors. However, in the case of six-electron formation, both the power and voltage are higher than in a system with only two-electron formation. This suggests that the increased number of electrons involved in the reaction enhances the overall energy output, thereby raising both power and voltage. When comparing the sharp decrease in voltage observed in Figure 2 with the behavior seen in the four-electron formation system, it is clear that the six-electron system behaves differently. The voltage decreases more gradually, indicating a more stable electron flow despite the increased number of electrons involved. The power output follows a similar trend as in the other systems, but with a notable difference in magnitude when compared to the two-electron formation system. This difference highlights the significant impact of electron formation on the system's performance. In systems with more electrons per reaction, the screening effect is less dominant, leading to more efficient energy conversion and higher power outputs. The nature of the power and voltage in the six-electron system suggests that increasing the number of electrons involved in the reaction can enhance system performance, particularly at lower current densities. Influence of fuel cell temperature on the performance of fuel cell. Under low current condition, the voltage output keeps decrease with the increase of working temperature. Under high current condition, higher working temperature makes the concentration losses reduced, resulting in higher voltage output [32].

Figure 7 illustrates the pronounced effects of both screening and temperature on power and voltage, deviating significantly from previous experimental work. The differences in power and voltage behavior are stark, indicating that the interplay between these factors can lead to unexpected outcomes in the system's performance. One particularly notable observation is the occurrence

of negative voltage, which is accompanied by negative power. This phenomenon suggests a fundamental shift in the behavior of the system under certain conditions. The emergence of negative voltage, often referred to as reverse voltage, implies that the direction of the potential difference across the system has reversed. In typical scenarios, voltage is positive, driving the flow of electrons through the circuit in a direction that supports energy generation. However, when the voltage becomes negative, it indicates that the system is experiencing a reverse bias, where the current is flowing in the opposite direction. This reverse flow can lead to energy being consumed rather than generated, resulting in negative power output. The occurrence of negative power is particularly significant, as it indicates that the system is absorbing energy instead of delivering it. This reversal in energy flow can be attributed to the screening effect, which becomes more pronounced when a larger number of electrons are formed in a single reaction. The screening effect involves the interaction of electric fields between closely spaced electrons, which can hinder their movement and create additional resistance to the flow of current. As a result, the system becomes less efficient in converting energy, and under certain conditions, this inefficiency leads to a net loss of energy, manifested as negative power. The intensity of the screening effect is directly related to the number of electrons involved in the reaction. When more electrons are generated in a single reaction, the screening effect increases, creating a stronger barrier to electron flow. This heightened resistance can lead to a scenario where the voltage drops into negative territory, and the power output follows suit. The relationship between electron formation, screening, and reverse voltage is critical in understanding how to optimize the performance of such systems.

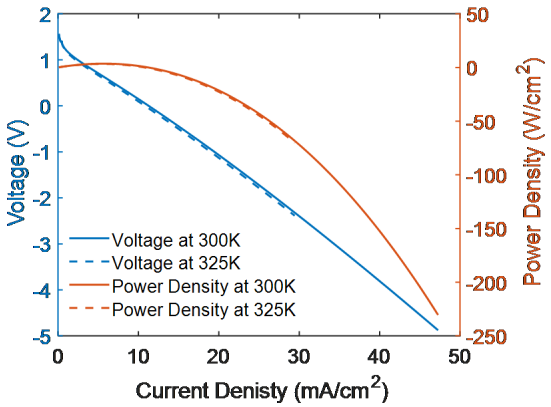

FIGURE 7. IV characteristic at 40 mV with 8 electrons per nano sec

The presence of negative voltage and power in Figure 7 suggests that the system is operating in a regime where the usual energy conversion processes are disrupted. This disruption could be due to several factors, including excessive electron formation leading to intense screening effects, or temperature conditions that exacerbate these effects. The negative voltage indicates that the potential barrier created by the screening effect is so strong that it overcomes the normal driving force of the reaction, causing the system to absorb energy rather than produce it. Understanding the implications of negative voltage and power is essential for optimizing electrochemical systems. In practical terms, these phenomena can reduce the overall efficiency of the system and may even lead to instability or failure if not properly managed. To mitigate these effects, it may be necessary to carefully control the number of electrons formed in the reaction, manage temperature conditions, or reduce the intensity of the screening effect through material or structural modifications. At the same current density and temperature, the activation potential plays a crucial role in determining the overall performance of the electrochemical system. Specifically, it was observed that an activation potential of 55 mV resulted in lower performance compared to a lower activation potential of 40 mV. This implies that a lower activation potential is more favorable for enhancing the system's efficiency and performance. As demonstrated in Figure 2, the performance of single cells deteriorated across the entire range of current densities after extended operation. The cells operated at temperatures of 65 °C and 90 °C for 100 hours showed a decrease in voltage from an initial value of 0.636 V to 0.615 V and 0.578 V, respectively. These voltage drops correspond to performance decay rates of 3.30% and 9.12% at 65 °C and 90 °C, respectively. The data indicates that higher temperatures accelerate the degradation of the PEMFCs. Several factors contribute to the observed performance degradation of Membrane Electrode Assemblies (MEAs). The performance and lifetime of MEAs are influenced by components such as membranes, platinum (Pt) catalysts, carbon supports, and GDLs [33]. While increasing the temperature can reduce the corrosion of carbon supports caused by water flooding, it simultaneously exacerbates the mechanical and chemical degradation of the membrane and increases the dissolution rate of Pt [34]. At elevated temperatures, such as 90 °C, the degradation mechanisms are more pronounced. The increased temperature accelerates the degradation of the membrane, leading to a more significant reduction in voltage compared to operation at 65 °C. The activation potential significantly impacts the performance of PEMFCs, with a lower activation potential being more beneficial. The performance degradation observed at higher temperatures underscores the importance of carefully managing operating conditions to balance the benefits of increased temperature with the potential for accelerated degradation of cell components. The findings suggest that while some temperature increases might al-

leviate specific issues, they generally lead to more severe performance losses due to enhanced degradation of critical components.

CONCLUSION

This research shows activation potential, current density, and temperature play an important role to determining the performance of Pt/C catalysts in PEMFCs. The activation potential shows lower activation potentials improved system performance when compared to higher potentials. The IV characteristic of PEMFC shows temperature play an important role. So careful management of activation potentials and operating temperatures to optimize fuel cell performance and prevent operational needed. The study contributes valuable insights into the complex interactions affecting PEMFCs and offers guidance for enhancing their efficiency and longevity through strategic adjustments to system parameters.

ACKNOWLEDGMENTS

We would like to express our sincere gratitude to the Central Department of Physics at Tribhuvan University, Kirtipur, Kathmandu, and the Department of Physics at Patan Multiple Campus, Tribhuvan University, Patandhoka, Lalitpur, Nepal, for their invaluable support throughout this study. We also extend our heartfelt appreciation to the University Grants Commission (UGC) for providing the necessary funding to conduct this research.

AUTHOR CONTRIBUTIONS

Saddam Husain Dhobi: Identify the problem, Design methodology, Analysis the result and write the paper.
Suresh Prasad Gupta and Kishori Yadav: Supervised, Validation and Review the work.
Jeevan Jyoti Nakarmi: Supervise, Validation and help Analysis and Interpretation.
Ajay Kumar Jha: Supervise, Review, Validation and help is technical part of paper.

EDITORS' NOTE

This manuscript was rigorously peer-reviewed and subsequently accepted for inclusion in the special issue of the Journal of Nepal Physical Society (JNPS) after it was submitted to the Association of Nepali Physicists in America (ANPA) Conference 2024.

REFERENCES

1. J. M. Jackson, M. L. Hupert, and S. A. Soper, "Discrete geometry optimization for reducing flow non-uniformity, asymmetry, and parasitic minor loss pressure drops in z-type configurations of fuel cells," Journal of Power Sources **269**, 274–283 (2014).
2. Y. Al-Okbi, A. S. N. Al-murshedi, M. N. Nemah, and H. A. K. Saad, "Influence of design anode and cathode channel on (pemfc) fuel cell performance," Materials Today: Proceedings **42**, 2177–2184 (2021).
3. Z. U. Bayrak and N. Celik, "Determining the effects of operating conditions on current density of a pemfc by using taguchi method and anova," Arabian Journal for Science and Engineering **49**, 10741–10752 (2024).
4. B. O. Emmanuel, P. Barendse, and J. Chamier, "Effect of anode and cathode reletive humidity variance and pressure gradient on single cell pemfc performance," in *2018 IEEE Energy Conversion Congress and Exposition (ECCE)* (IEEE, 2018) pp. 3608–3615.
5. J. Baschuk and X. Li, "Modeling of ion and water transport in the polymer electrolyte membrane of pem fuel cells," International journal of hydrogen energy **35**, 5095–5103 (2010).
6. S. Tzelepis, K. A. Kavadias, G. E. Marnellos, and G. Xydis, "A review study on proton exchange membrane fuel cell electrochemical performance focusing on anode and cathode catalyst layer modelling at macroscopic level," Renewable and Sustainable Energy Reviews **151**, 111543 (2021).
7. V. A. Sethuraman, J. W. Weidner, A. T. Haug, S. Motupally, and L. V. Protsailo, "Hydrogen peroxide formation rates in a pemfc anode and cathode: Effect of humidity and temperature," Journal of The Electrochemical Society **155**, B50 (2007).
8. M. Danilczuk, F. D. Coms, and S. Schlick, "Visualizing chemical reactions and crossover processes in a fuel cell inserted in the esr resonator: detection by spin trapping of oxygen radicals, nafion-derived fragments, and hydrogen and deuterium atoms," The Journal of Physical Chemistry B **113**, 8031–8042 (2009).
9. R. Singh, P. Sui, K. Wong, E. Kjeang, S. Knights, and N. Djilali, "Modeling the effect of chemical membrane degradation on pemfc performance," Journal of The Electrochemical Society **165**, F3328–F3336 (2018).
10. Y.-G. Zhou, Y. Kang, and J. Huang, "Fluidized electrocatalysis," CCS Chemistry **2**, 31–41 (2020).
11. M. Qiao, Y. Wang, Q. Wang, G. Hu, X. Mamat, S. Zhang, and S. Wang, "Hierarchically ordered porous carbon with atomically dispersed fen4 for ultraefficient oxygen reduction reaction in proton-exchange membrane fuel cells," Angewandte Chemie International Edition **59**, 2688–2694 (2020).
12. R. A. Venegas Toledo, K. Muñoz Becerra, C. Candia Onfray, J. F. Marco Sanz, J. H. Zagal Moya, and F. J. Recio Cortés, "Experimental reactivity descriptors of mnc catalysts for the oxygen reduction reaction," (2020).
13. X. Wang, J. Fang, X. Liu, X. Zhang, Q. Lv, Z. Xu, X. Zhang, W. Zhu, and Z. Zhuang, "Converting biomass into efficient oxygen reduction reaction catalysts for proton exchange membrane fuel cells," Science China Materials **63**, 524–532 (2019).
14. X. Huang, T. Shen, T. Zhang, H. Qiu, X. Gu, Z. Ali, and Y. Hou, "Efficient oxygen reduction catalysts of porous carbon nanostructures decorated with transition metal species," Advanced Energy Materials **10**, 1900375 (2020).
15. X. Cai, R. Lin, D. Shen, and Y. Zhu, "Gram-scale synthesis of well-dispersed shape-controlled pt- ni/c as high-performance catalysts for the oxygen reduction reaction," ACS applied materials & interfaces **11**, 29689–29697 (2019).
16. S. Dhali, M. Karakoti, S. Pandey, B. SanthiBhushan, R. K. Verma, A. Srivastava, R. Bal, S. Mehta, and N. G. Sahoo, "Graphene oxide supported pd-fe nanohybrid as an efficient electrocatalyst for proton exchange membrane fuel cells," International Journal of Hydrogen Energy **45**, 18704–18715 (2020).

17. O. T. Holton and J. W. Stevenson, "The role of platinum in proton exchange membrane fuel cells," Platinum Metals Review **57**, 259–271 (2013).
18. L. Yang, Z. Sun, G.-M. Zhang, Z.-S. Li, and K.-X. Ren, "Unmasking the reactants inhomogeneity in gas diffusion layer and the performances of pemfc induced by assembly pressure," Heliyon **10** (2024).
19. K. Aliyah, C. Appel, T. Lazaridis, C. Prehal, M. Ammann, L. Xu, M. Guizar-Sicairos, L. Gubler, F. N. Buchi, and J. Eller, "Operando scanning small-/wide-angle x-ray scattering for polymer electrolyte fuel cells: Investigation of catalyst layer saturation and membrane hydration–capabilities and challenges," ACS Applied Materials & Interfaces (2024).
20. H. Yu, M. J. Zachman, K. S. Reeves, J. H. Park, N. N. Kariuki, L. Hu, R. Mukundan, K. C. Neyerlin, D. J. Myers, and D. A. Cullen, "Tracking nanoparticle degradation across fuel cell electrodes by automated analytical electron microscopy," ACS nano **16**, 12083–12094 (2022).
21. C. Roth, N. Benker, T. Buhrmester, M. Mazurek, M. Loster, H. Fuess, D. C. Koningsberger, and D. E. Ramaker, "Determination of o [h] and co coverage and adsorption sites on ptru electrodes in an operating pem fuel cell," Journal of the American Chemical Society **127**, 14607–14615 (2005).
22. E. B. Lehman, "Electrochemistry for materials science," Lecture Note (2021) institute of Metallurgy and Materials Science Polish Academy of Sciences, Poland.
23. H. Najafizadegan and H. Zarabadipour, "Control of voltage in proton exchange membrane fuel cell using model reference control approach," International Journal of Electrochemical Science **7**, 6752–6761 (2012).
24. Y. Akimoto and K. Okajima, "Semi-empirical equation of pemfc considering operation temperature," Energy Technology & Policy **1**, 91–96 (2014).
25. J. R. Esquius and L. Liu, "High entropy materials as emerging electrocatalysts for hydrogen production through low-temperature water electrolysis," Materials Futures **2**, 022102 (2023).
26. N. Bizon, "On tracking robustness in adaptive extremum seeking control of the fuel cell power plants," Applied Energy **87**, 3115–3130 (2010).
27. K. Ermis, E. Toklu, and M. Yegin, "Investigation of operating temperature effects on pem fuel cell," Journal of Engineering Research and Applied Science **9**, 1538–1545 (2020).
28. N. Sezer, S. Bayhan, U. Fesli, and A. Sanfilippo, "A comprehensive review of the state-of-the-art of proton exchange membrane water electrolysis," Materials Science for Energy Technologies (2024).
29. J. Zhao, X. Huang, H. Chang, S. H. Chan, and Z. Tu, "Effects of operating temperature on the carbon corrosion in a proton exchange membrane fuel cell under high current density," Energy Conversion and Management: X **10**, 100087 (2021).
30. I. A. Soomro, F. H. Memon, W. Mughal, M. A. Khan, W. Ali, Y. Liu, K. H. Choi, and K. H. Thebo, "Influence of operating and electrochemical parameters on pemfc performance: A simulation study," Membranes **13**, 259 (2023).
31. A. R. V. Babu, P. M. Kumar, and G. S. Rao, "Parametric study of the proton exchange membrane fuel cell for investigation of enhanced performance used in fuel cell vehicles," Alexandria engineering journal **57**, 3953–3958 (2018).
32. Z. Song, Y. Pan, H. Chen, and T. Zhang, "Effects of temperature on the performance of fuel cell hybrid electric vehicles: A review," Applied Energy **302**, 117572 (2021).
33. S. Zhang, X. Yuan, H. Wang, W. Mérida, H. Zhu, J. Shen, S. Wu, and J. Zhang, "A review of accelerated stress tests of mea durability in pem fuel cells," International journal of hydrogen energy **34**, 388–404 (2009).
34. X.-Z. Yuan, H. Li, S. Zhang, J. Martin, and H. Wang, "A review of polymer electrolyte membrane fuel cell durability test protocols," Journal of Power Sources **196**, 9107–9116 (2011).